World Journal of Advanced Research and Reviews
eISSN: 2581-9615 CODEN (USA): WJARAI
Cross Ref DOI: 10.30574/wjarr
Journal homepage: https://wjarr.com/

(RESEARCH ARTICLE)

Check for updates

Method of locating a target with a Mimo radar distributed at the international airport of Ndjili in Kinshasa

Joséphine Mpole Boyokame [1], Ch. G. Lionel Nkouka Moukengue [2], Flory Lidinga Mobonda [2, 1], N. Meni Babakidi [1], J. G. Cimbela Kasongo [1] and Maguiraga Madiassa [1]

[1] *Laboratory of Electrical and Electronic Engineering, UPN-Kinshasa, Democratic Republic of Congo.*
[2] *Laboratory of Electrical and Electronic Engineering, ENSP, Marien Ngouabi University, Congo.*

World Journal of Advanced Research and Reviews, 2023, 18(02), 952–960

Publication history: Received on 12 April 2023; revised on 19 May 2023; accepted on 21 May 2023

Article DOI: https://doi.org/10.30574/wjarr.2023.18.2.0900

Abstract

In this article, we address the probability of target localization from a MIMO radar at Ndjili International Airport. This article describes a target detection and localization system.
This system is based on a UWB wave distributed radar using a trilateration algorithm for localization. Before describing the complete system, we detail some signal processing techniques on the UWB signals acquired directly at the output of the reception antenna. To apply the trilateration algorithm, the signals coming from the reception antennas must first be shaped. The necessary processing is to improve the signal to noise ratio (S/N), to extract the signal envelope and to determine the propagation time. Once the propagation time is known, the trilateration algorithm is used to locate the targets.

Keywords: Locating a target; MIMO Radar; International Airport of Ndilli; Kinshasa

1. Introduction

In recent years, a new type of antenna system, multiple-input multiple-output (MIMO), has been introduced [1,2]. A MIMO antenna system is generally defined as a system that has multiple transmitted linearly independent waveforms and is capable of jointly processing multiple received antenna signals. MIMO radar draws on the idea of MIMO communication. MIMO radars can be classified into two main classes according to the arrangement of its transmitters and receivers elements. The first class is the known as "statistical radar" whose elements are widely spaced.

The second is the radar consisting of multiple co-located transmit antennas and multiple co-located receive antennas [3,4,5,6,7].

The detection processes that constitute a chain of operations are the basis of any radar system application. Detection at the receiver consists of determining the presence or absence of a target based on a set of observations resulting from the received signal. Associated with computers that rapidly process the information received and transform it for immediate visualization and exploitation, radar is more than ever the basis of air surveillance systems.

Despite the existence of the radar signal detection circuit and the permanent surveillance devices in the airports, the radar signal detection system and the estimation of their arrival times still pose serious problems.

This is why the modernization of airports and the construction of adequate control towers remain an urgent necessity in the airports of the Democratic Republic of Congo in general and the international airport of N'djili in particular in order to explore and analyze the different techniques of radar signal detection and target location.

* Corresponding author: Lionel Nkouka Moukengue

The most classical techniques for locating a target use the geometry of triangles [8,9,10]. Among these methods, the trilateration and triangulation techniques are the most widely used. For the latter, the distances are calculated from the observed angles (AoA), while for trilateration, the target is located from the observed distances.

This last technique is often used in the field of navigation (in particular for GPS) or for the search of people. In a 2D space, two reference points are sufficient to determine the localization, the addition of reference points makes it possible to increase the precision of the localization.

In the case of aerospace location, signal propagation does not occur in a straight line. This makes it tricky to use the triangulation technique. We therefore preferred to use localization techniques based on trilateration.

2. Radar geometric methods

Several numerical methods exist. The best known is Newton's method. It is an efficient algorithm for finding an accurate approximation of a zero (or root) of a real function of a real variable. The main interest of Newton's algorithm is its local quadratic convergence. A more robust method is that proposed by Brent-Dekker. It is an approach combining dichotomy, secant method and inverse quadratic interpolation. It is also faster, and it happens to be very accurate.

In practice, it is very rare to have only 2 receivers. Often the bistatic radars have at least 3 receivers which requires, to locate the target, to define the zone of intersection of three circles. The method described below can be generalized.

2.1. Location of target P

The complexity of the problem lies in the systematic existence of measurement uncertainty on the coordinates of the sensors and on the measured distances as shown in figures 1 and 2. These make the problem analytically insoluble, thus requiring the use of numerical techniques. Two methods are classically used to solve this problem: geometric (analytical) methods and statistical (numerical) methods.

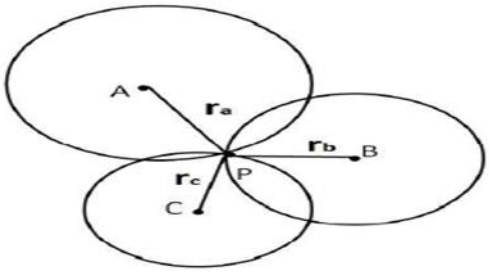

Figure 1 Location of the target P, without measurement uncertainty on r_a, r_b, r_c.

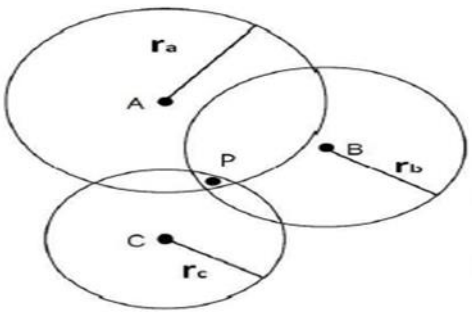

Figure 2 Location of target P, with measurement uncertainties on r_a, r_b, r_c.

2.2. Intersection by two circles

To illustrate this method, let us detail the geometric method in the simple case where there are only 2 receivers. The objective is to determine the central zone of the union of 2 circles C_A and C_B, with

center A (x_a , y_a) and B (x_b , y_b) respectively, with radius r_a and r_b (figure 3). These 2 circles intersect at D (x_d , y_d) and E (x_e , y_e). We calculate the barycenter C of the zone common to C A and C B according to the following method (we assume $r_a < rb\_$ and A ≠ B).

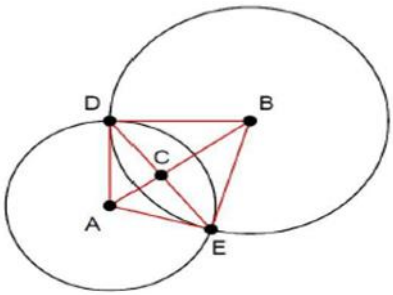

Figure 3 Intersection of the two circles.

2.3. **Intersection by three circles**

Let 3 circles, C_A (A, r_a) , C_B (B, r_b) and C_C (C, r_c) whose union defines an area of intersection, instead of a single point, of the there are measurement uncertainties. The objective is to find the zone of intersection (ZI) common to the three circles which corresponds to the location of the target as illustrated in Figure 4.

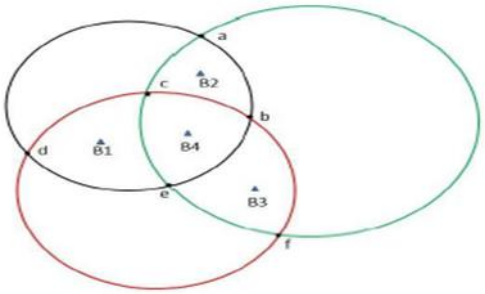

Figure 4 B1: barycenter of the intersection zone c,e,d ; B2: barycenter of the intersection zone a,b,c ; B3: barycenter of the intersection zone b,e,f ; B4: barycenter of the intersection zone b,c,e.

3. Equation d'intersection des cercles

3.1. Angle of Arrival (AOA)

In this method, the distance is obtained by determining the direction of wave propagation using an antenna array. Figure 5 shows the localization by AOA measurement.

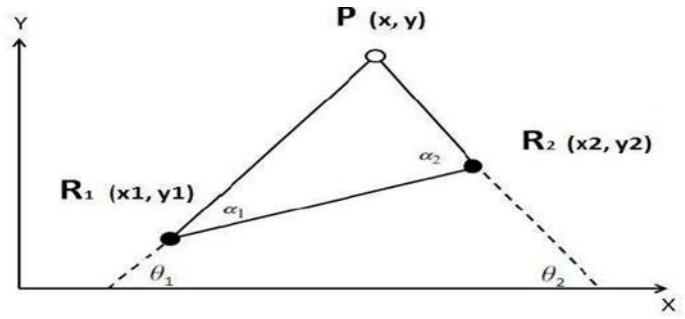

Figure 5 Location by AOA measurement.

The white point P(x,y) represents the target to be detected, the sensors are represented by black points Ri(xi,yi) with i = 1,2,3...N. αi represents the angle that the direction of arrival of the signal makes with the sensor array. θi is the angle formed by the target and the sensor Ri with respect to the X axis. In a Cartesian reference frame, we express this angle by the following relation:

$$tan\big(\theta_i(P)\big) = \frac{y - y_i}{x - x_i}, 1 \le i \ll n \qquad (1)$$

It is assumed that the measurement of αi is tainted by an error εi that can be modeled by additive white Gaussian noise [11] of variance σ^2_i :

$$\alpha_i = \theta_i(P) + \varepsilon_i, 1 \le i \ll n \qquad (2.2)$$

If the reference sensors are identical and are located close enough to the target to be detected, the variances of the measurement errors are identical: $\sigma^2_i = \sigma^2$, $1 \le i \le n$. The maximum likelihood estimator of the target location is given by the formula (2):

$$\hat{P}(x, y) = \arg min \frac{1}{2} \sum_{i=1}^{n} \frac{(\theta_i(P) - \alpha_i)^2}{{\sigma_i}^2} \qquad (2)$$

This nonlinear minimization problem can be solved by the Newton-Gauss algorithm [12]. If the measurement error is small enough, εi can be approximated and expressed as sin (εi). In this case, equation (2) becomes:

$$\hat{P}(x, y) = \arg min \frac{1}{2} \sum_{i=1}^{n} \frac{(sin^2\theta_i(P) - \alpha_i)}{{\sigma_i}^2} \qquad (3)$$

The solution of this equation can be calculated analytically in the form of a matrix calculation. The distance between the sensor and the target is given by the formula (4):

$$d_i = \sqrt{(x_0 - x_i)^2 + (y_0 - y_i)^2} \qquad (4)$$

$$sin(\theta_i(P) - \alpha_i) = sin\big(\theta_i(P)\big)cos\alpha_i - cos\big(\theta_i(P)\big)sin\alpha_i = \frac{(y_0 - y_i)cos\alpha_i - (x_0 - x_i)sin\alpha_i}{d_i} \qquad (5)$$

So the equation becomes:

$$\frac{1}{2} \sum_{i=1}^{n} \frac{[(y_0 - y_i)cos\alpha_i - (x_0 - x_i)sin\alpha_i]^2}{{\sigma_i}^2 {d_i}^2} = \frac{1}{2}(A \to x - b)^T R^{-1} S^{-1} (A \to x - b) (6)$$

$$A = \begin{bmatrix} sin\alpha_1 & -cos\alpha_1 \\ \dots & \dots \\ sinn & -cos\alpha_n \end{bmatrix} \qquad (7)$$

$$h = \begin{bmatrix} x_1 sin\alpha_1 & -y_1 cos\alpha_1 \\ \dots & \dots \\ x_n sinn & -y_n cos\alpha_n \end{bmatrix} \qquad (8)$$

3.2. Two-circle method

First, we calculate the distance △ between the centers of the two circles by the formula (9):

$$\Delta = \sqrt{(x_0 - x_i)^2 + (y_0 - y_i)^2} \qquad (9)$$

The calculation of the coordinates of C(xc, yc) requires the calculation of the distances AC, noted s, BC, noted t, CD and CE noted u.

$$s^2 + u^2 = {r_a}^2 \qquad (10)$$

$$t^2 + u^2 = {r_b}^2 \qquad (11)$$

The difference of equations (10) and (11) gives:

$$(s - t)(s + t) = {r_a}^2 - {r_b}^2 \qquad (12)$$

But t=Δ-s, we therefore obtain:

$$s = \frac{\Delta^2 + {r_a}^2 + {r_b}^2}{2\Delta} \qquad (13)$$

$$\left(x_x + \frac{u.\Delta_y}{\Delta}, y_c - \frac{u.\Delta_x}{\Delta}\right) \qquad (14)$$

3.3. Hilbert transform

The Hilbert transform was then applied, in order to "demodulate" the signal, to recover only its envelope. We note H the Hilbert transform of a real variable function. The Hilbert transform of the signal s(t) is obtained by convolving the signal s(t) with 1/πt, and is denoted ˆs(t). The Hilbert transform s(t) can be interpreted as the output of a linear invariant system of impulse response 1/πt, excited by the input s(t). It is a mathematical tool widely used in signal theory to describe the complex envelope of a real quantity modulated by a signal. The Hilbert transform is defined as:

$$\hat{s}(t) = H\{s\} = (h * s)(t) = vp\left\{\int_{-\infty}^{\infty} s(\tau)h(t-\tau)d\tau\right\} = \frac{1}{\pi} vp\left\{\int_{-\infty}^{\infty} \frac{s(\tau)}{t-\tau} d\tau\right\} \quad (15)$$

Or

$$h(t) = \frac{1}{\pi t} \qquad (16)$$

$$vp\left\{\int_{-\infty}^{\infty} s(\tau)h(t-\tau)d\tau\right\} = \lim_{\epsilon \to 0}\left\{\int_{-\infty}^{t-\epsilon} s(\tau)h(t-\tau)d\tau + \int_{t+\epsilon}^{\infty} s(\tau)h(t-\tau)d\tau\right\} \quad (17)$$

4. Results and discussion

4.1. Acquisition system

The signal acquisition chain consists of a pulson UWB transmitter 201, which emits a pulse, the time course of which is represented by a raw signal, measured directly at the output of the antenna via the oscilloscope figure 6. Such a signal without a minimum of processing is totally unusable.

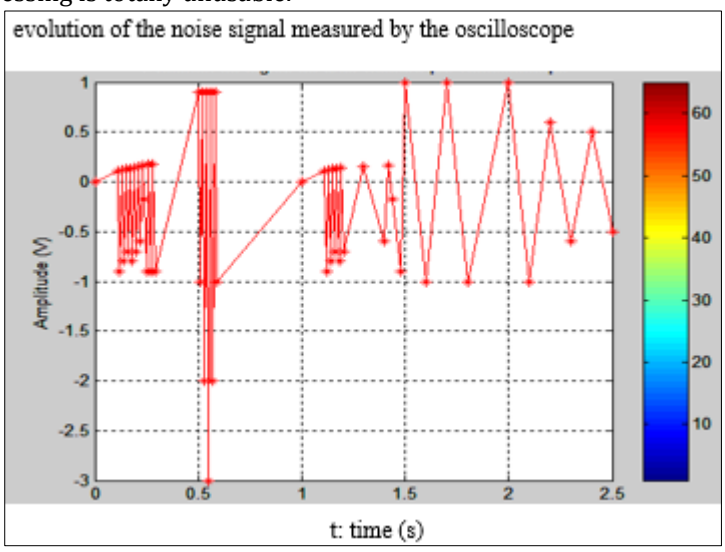

Figure 6 Noise signal measured by the oscilloscope

4.2. Averaging method

The first processing must improve the signal to noise ratio. The simplest method is to average several acquisitions. Figures 7, 8, 9 and 10 show the improvement in S/N for different averages performed directly by the oscilloscope (4, 16, 64, 256). We can see very clearly the echo of the target from an averaging on 4 signals.

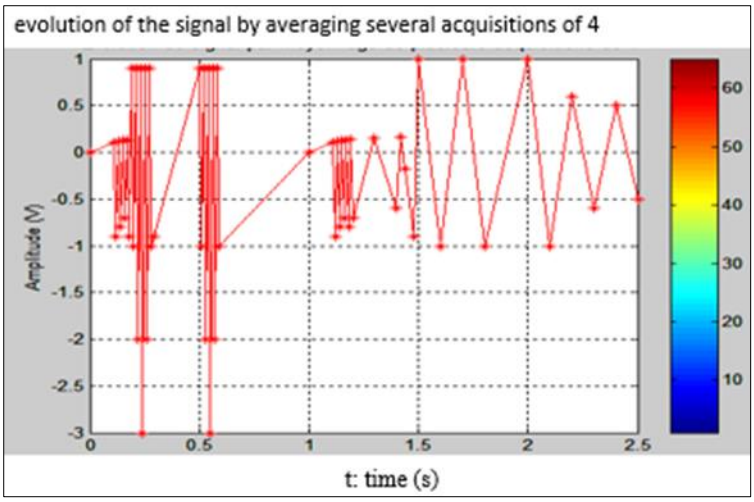

Figure 7 Signal after processing by averaging several acquisitions (average of 4).

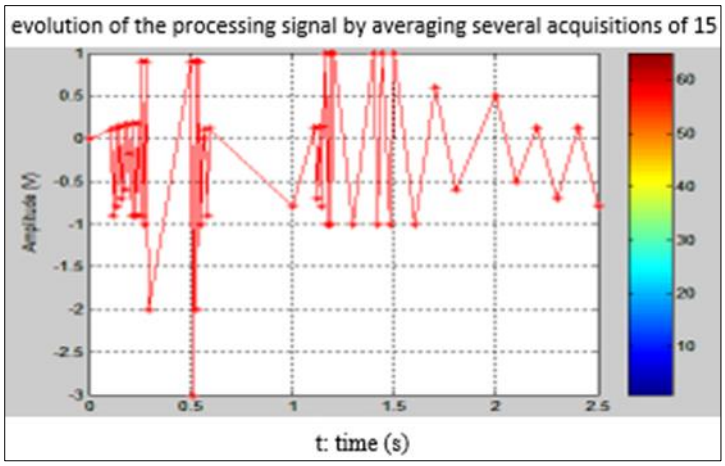

Figure 8 Signal after processing by averaging several acquisitions (average of 16).

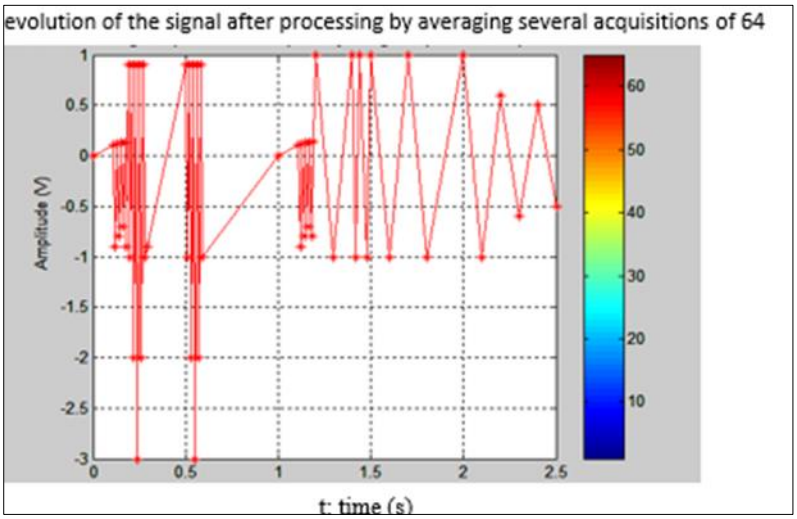

Figure 9 Signal after processing by averaging several acquisitions (average of 64)

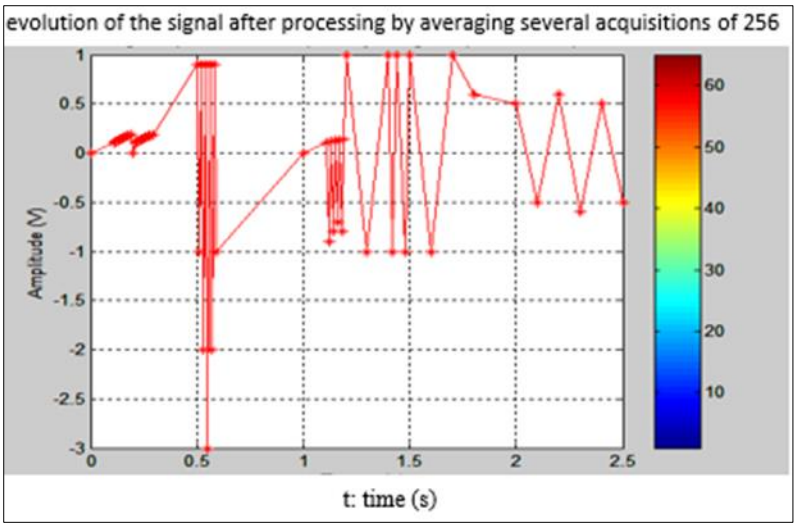

Figure 10 Signal after processing by averaging several acquisitions (average of 256).

Given that the amplitude of the direct coupling is much larger than that of the target echo, in the following treatments and algorithms proposed, we keep only the part of the signal related to the target echo in order to avoid a "crushing" of this echo. Figure 11 represents the received signal with an average of 256 where the direct coupling has been removed, by subtraction with a reference signal without target.

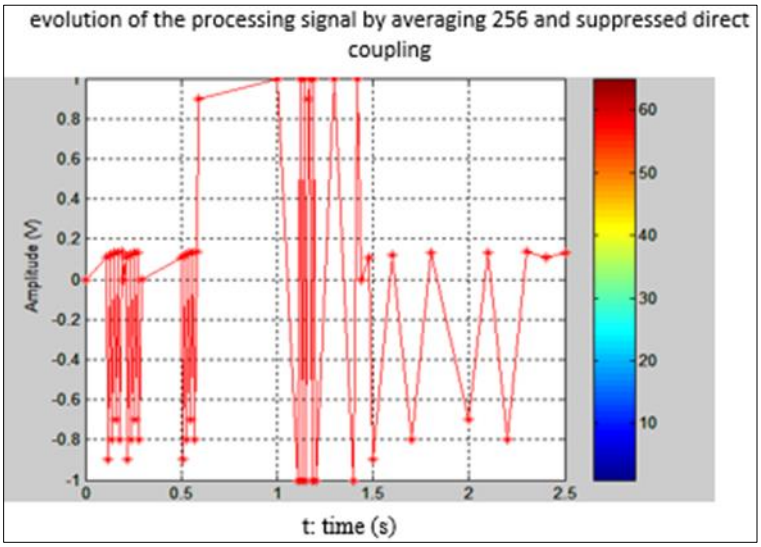

Figure 11 Signal after processing by averaging of 256 signals and direct coupling removed)

4.3. Hilbert transform

At the end of these treatments, the peak of the target signal appears clearly, which makes it possible to determine the propagation time of the signal (figure 12). However, the first processing corresponding to the averaging is relatively long (it depends on the number of averaged signals) and is therefore not easily compatible with a real-time processing. Therefore, we have proposed another method to extract the signal from the noise using a technique based on the calculation of higher order moments (MOS).

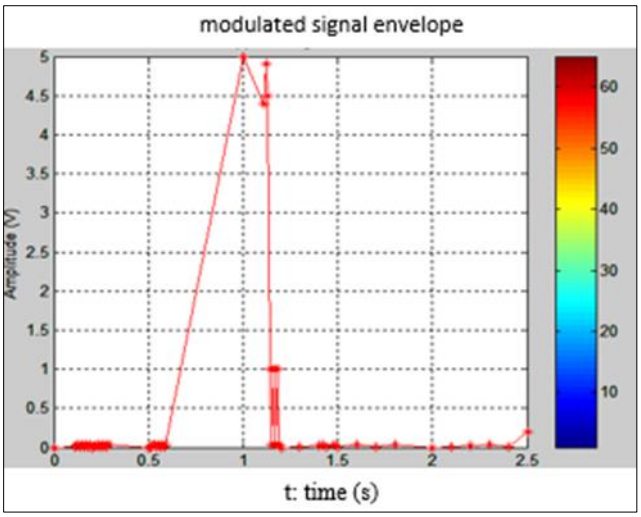

Figure 12 Envelope of the modulated signal.

5. Conclusion

We saw that this article was about locating a target from the multiple input multiple output (MIMO) radar in the international airport of Ndjili. Based on the latter configuration, which appears to be an excellent compromise between complexity, gains related to coherence and gains related to spatial diversity, and on high-resolution source localization methods, we have proposed some approaches for joint localization of arrival and departure directions of targets. These approaches decompose the two-dimensional search for directions into two one-dimensional searches, which significantly reduces the computational complexity. The radar signal is often modulated in binary phase which motivated us to take into consideration this property of non-circularity. Indeed, this property allows us to offer another degree of diversity in addition to those provided by the MIMO concept.

Compliance with ethical standards

Disclosure of conflict of interest

No conflict of interest.

References

[1] Sharma, P.; Tiwari, R.N.; Singh, P.; Kumar, P.; Kanaujia, B.K. MIMO Antennas: Design Approaches, Techniques and Applications. Sensors 2022, 22, 7813.

[2] Hu, X.; Tong, N.; Wang, J.; Ding, S.; Zhao, X. Matrix completion-based MIMO radar imaging with sparse planar array. Signal Process. 2017, 131, 49–57

[3] Zhi Dong, Zheng Jian, Yun Zhang, Peng Ma Chun, and Sheng Liu. Angle estimation with automatic pairing for bistatic MIMO radar pages pages 1-5 Tianjin, October 2009.

[4] C. Duofang, C. Baixiao, and Q. Guodong. Angle estimation using ESPRIT in mimo radar. Electronics Letters, 44(12) :770-771, 2008. (Cité en pages 2, 24, 25, 32, 36 et 38.)

[5] E. Fishler, A. Haimovich, R. Blum, D. Chizhik, L. Cimini, and R. Valenzuela. MIMO radar : An idea whose time has come. In Radar Conference, 2004. Proceedings of the IEEE, pages 71-78, 2004. (Cité en pages 2 et 16.)

[6] E. Fishler, A. Haimovich, R. Blum, R. Cimini, D. Chizhik, and R. Valenzuela. Performance of MIMO radar systems : Advantages of angular diversity. In Signals, Systems and Computers, 2004. Conference Record of the Thirty-Eighth Asilomar Conference on, volume 1, pages 305-309, 2005. (Cité en page 2.)

[7] Jian Li and Petre Stoica. MIMO radar signal processing. John Wiley & Sons, Inc., 2010.

[8] H. Godrich, A. M Haimovich, and R. S Blum. Target localization techniques and tools for MIMO radar. In Radar Conference, 2008. RADAR'08. IEEE, pages 1-6, 2008.

[9] Yongwei Zhang , Yongchao Zhang , Jiawei Luo , Yulin Huang, Jianan Yan , Yin Zhang and Jianyu Yang '' An ADMM-qSPICE-Based Sparse DOA Estimation Method for MIMO Radar'' remote sensing, 11 january 2023

[10] Yongqiang Cheng *, Xiaoqiang Hua, Hongqiang Wang, Yuliang Qin and Xiang Li '' The Geometry of Signal Detection with Applications to Radar Signal Processing'' Entropy 2016, 18, 381

[11] C. Yunhe. Joint estimation of angle and doppler frequency for bistatic MIMO radar. Electronics Letters, 46(2) :170-172, 2010.

[12] Sie Long Kek, Jiao Li, Wah June Leong, Mohd Ismail Abd Aziz '' A Gauss-Newton Approach for Nonlinear Optimal Control Problem with Model-Reality Differences'' Open Journal of Optimization Vol.6 No.3, September 2017